J Mater Sci (2006) 41:7406–7412
DOI 10.1007/s10853-006-0800-6

Organoclay effect on transverse compressive strength of glass/epoxy nanocomposites

Jia-Lin Tsai · Jui-Ching Kuo · Shin-Ming Hsu

Received: 3 June 2005 / Accepted: 30 November 2005 / Published online: 20 September 2006

Abstract This research focuses on the fabrication of glass fiber/epoxy nanocomposites containing organoclay as well as understanding the organoclay effect on the transverse compressive strength of nanocomposites. To demonstrate the organoclay effect, three different loadings of organoclay were dispersed, respectively, in the epoxy resin using a mechanical mixer followed by sonication. The corresponding glass/epoxy nanocomposites were produced by impregnating dry glass fiber with organoclay epoxy compound through a vacuum hand lay-up procedure. Unidirectional block specimens were employed for transverse compression tests on a hydraulic MTS machine. Experimental observations indicate that glass/epoxy nanocomposites containing organoclay exhibit higher transverse compressive strength than conventional composites. Furthermore, the failure mechanisms for all tested specimens were found to be fiber and matrix debonding. Therefore, results indicate that the increasing characteristic in transverse failure stress may be ascribed to the enhanced fiber/matrix adhesion modified by the organoclay.

Introduction

Transverse compressive strength is of concern in the design of composite structures because its value is significantly low in comparison to other mechanical properties. Collings [1] measured the transverse compressive strength of carbon fiber reinforced plastics with different fiber volume fractions. His observations revealed that transverse compressive failure was mainly controlled by the fiber and matrix interfacial bonding. Bazhenov and Kozey's [2] investigations of transverse compressive failure of the fiber-reinforced composites indicated that the main failure mechanism was the transverse shearing taking place on the plane orientated approximately 35°–41° to the loading direction. Similar shearing failure was also observed by Lowe [3] when he performed transverse compression tests on T300/914 carbon/epoxy unidirectional composites at various strain rates and temperatures. In view of these studies, the transverse compressive fracture of fiber composites is controlled by transverse shearing, which basically is a matrix dominant property. For polymeric composites, the research implies that transverse compressive strength can be enhanced effectively if matrix properties as well as adhesive bonding to the fibers are improved.

With the characteristics of superior stiffness and strength as well as higher aspect ratio, nano-materials are considered to be superior reinforcement for improving matrix properties [4, 5]. Polymer reinforced with organoclay platelets is one particular class of nanocomposites that has attracted considerable attention since Toyota researchers successfully improved the mechanical properties of nylon6 a decade ago [6, 7]. The organoclay platelet is an ultra-thin (1 nm) silicate film with lateral dimensions up to 1 μm. Without special treatments, the platelets are held together by the weak ionic bond with clay tactoids, and gallery spacing of interlayer is less than 1 nm. Through the ion

J.-L. Tsai (✉) · J.-C. Kuo · S.-M. Hsu
Department of Mechanical Engineering, National Chiao Tung University, Hsinchu 300, Taiwan
e-mail: jialin@mail.nctu.edu.tw

exchange processing, sodium ions attracted on the surfaces of the platelets are replaced with organic cations, which can improve the interfacial adhesion between the polymer and the platelet and facilitate the exfoliation of the organoclay. After an appropriate fabrication procedure, i.e. melt compounding [8], in situ polymerization [9, 10] and solution method [11], the aggregated platelets can be exfoliated and dispersed uniformly in the polymer. Depending on the degree of exfoliation, three different categories of nanocomposites—tactoids, intercalated and exfoliated—can be produced [12]. For tactoids, the clay platelets are still aggregated together, and no polymer molecule moves into the galleries of the adjacent platelets. For intercalated nanocomposites, one or more molecular layers of polymer are inserted into the galleries of the platelets, and gallery spacing becomes 2–3 nm. When more polymer molecules move into the galleries resulting in further separation of the platelets, the exfoliated nanocomposites take place. In general, in this case, gallery spacing is around 8 nm or more. It is desirable to have dispersed and exfoliated organoclay in the nanocomposites since experimental observations indicate that the stiffness of nanocomposites can be enhanced significantly if the platelets are well dispersed in epoxy resin [8, 13].

In past decades, most of the effort related to nanocomposites was made on the polymers and their organoclay compounds while few works concerning organoclay effects on conventional fiber composites have been carried out. Haque et al. [14] investigated interlaminar shear strength, flexural properties and fracture toughness for both conventional glass/epoxy composites and glass/epoxy nanocomposites with low loadings of organoclay. Results indicate that with dispersing 1 wt% organoclay, the glass/epoxy nanocomposites demonstrated 44% improvement on interlaminar shear strength as compared to the conventional composites. Becker et al. [15] performed three point bending tests on ternary carbon fiber/epoxy/clay nanocomposites for the measurements of interlaminar shear strength. However, no significant improvement on interlaminar shear strength was found in the nanocomposites. So far, the literature regarding the organoclay effect on the mechanical behaviors of fiber/epoxy nanocomposites is still lacking.

This study aims to investigate the organoclay effects on the behavior of the epoxy resin as well as the corresponding fiber/epoxy nanocomposites. More attention will be paid to the influence of organoclay on transverse compressive failure since it is a matrix dominant property. Epoxy resin containing 2.5, 5 and 7.5% of weight of organoclay was fabricated and then tested in tension. The degree of exfoliation of organoclay dispersed in the epoxy resin was investigated using X-ray diffraction (XRD) and a transmission electron microscope (TEM). In order to produce transverse compressive failure, unidirectional block fiber/epoxy nanocomposites with various organoclay concentrations were prepared and then tested in the transverse direction. The failure mechanisms of the specimens were examined using a scanning electron microscope (SEM), and the failure stresses were measured in accord with different organoclay loadings.

Material preparation

Epoxy/organoclay nanocomposites

The epoxy resin used in this study is diglycidyl ether of bisphenol A (DGEBA, EPON828 with an epoxy equivalent weight of 187) supplied by Resolution Performance Products. The curing agent is polyoxypropylenediamine (Jeffamine D-230 with a molecular weight of 230) provided by Huntsman Corporation. The clay used for the synthesis of nanocomposites is organoclay (Nanomer I.30E) obtained from Nanocor, Inc. It is basically an octadecyl-ammonium ion surface modified montmorillonite mineral designed to be easily dispersed into amine-cured epoxy resin and to form nanocomposites as well [16]. When preparing the epoxy/clay nanocomposite samples, the organoclay clay was dried in the vacuum oven for 6 h at 90 °C in order to remove moisture and then blended with EPON828 at 80 °C for 4 h using a mechanical stirrer. The mixture was then sonicated using a sonicator with a cooling system around the sample container until the compounds became transparent. It should be noted that sonication is an ultrasonic liquid processing. In the liquid compound, microscopic bubbles are formed momentarily and then implode by means of ultrasonic vibration. The collapse of the thousands of bubbles can cause powerful shock waves to radiate throughout the sample resulting in clay platelet separation. The epoxy/clay mixture was degassed at room temperature in a vacuum oven for 10 min and mixed with a curing agent (32 wt% of EPON828). The mechanical stirrer was again utilized to blend the final mixture at room temperature for 10 min. To form the nanocomposite specimens for tensile tests, the mixture was poured into a specially designed steel mold with Teflon coating on its surfaces. Subsequently, the samples were cured at 100 °C for 3 h with an additional 3 h at 125 °C for post-curing. In the study, the nanocomposites containing 2.5, 5 and 7.5% loadings (by weight) of organoclay

were prepared, respectively. It should be noted that when nanocomposites contain high organoclay loading, viscosity becomes higher and retard the degassing process. More degassing time is required to effectively eliminate the embedded bubbles.

Glass fiber/epoxy nanocomposite

Vacuum-assisted hand lay-up procedures were adopted for preparing the glass fiber/epoxy nanocomposites. The final mixture of organoclay/epoxy together with the curing agent prepared as described previously was poured onto one dry unidirectional glass fiber layer (provided by Vectorply®, E-LR0908-14 unidirectional E-glass fiber). The dry fiber was impregnated with the resin using a hand roller. Then another ply of dry fiber was stacked on it. This process continued repeatedly until 18 layers of glass fiber nanocomposites were fabricated. The fiber stack was sandwiched between two steel plates with porous Teflon fabric on the surface and then sealed within a vacuum bag. The whole laminates were cured in a hot press at the suggested temperature profile with vacuum conditions. The vacuum is essential for forming nanocomposites since it can facilitate the removal of tiny bubbles trapped in the nanocomposites during the process. However, when the nanocomposites contain high organoclay loading (7.5 wt%), it is still a challenge to fully remove the bubbles even though the vacuum system is applied.

Material characterization

In order to evaluate the degree of exfoliation of the organoclay in the epoxy resin, the samples were examined using XRD and TEM, both of which are widespread methods for characterizing nanocomposites. XRD measurements were conducted on neat epoxy and epoxy/clay nanocomposites films (about 4 mm thick) using a Bede D1 diffractometer. The incident X-ray wavelength was 1.54 Å, and the scanning step size was 0.08°. Figure 1 shows the XRD patterns for the nanocomposites containing various loadings of organoclay as well as the organoclay and pure epoxy resin. For organoclay, the reflection peak is detected at $2\theta = 3.78°$ corresponding to the 2.3 nm interlayer spacing (d-spacing). However, there is no significant peak value found in the nanocomposites, which may be attributed to the fact that some clay platelets may not exhibit significant basal reflections and the intensity pattern, nor are their relative peaks easily detected [17]. Thus, the XRD pattern may not be a full indication of the morphology of the nanocomposites. To further understand the morphology of the nanocomposites, we resort to the assistance of the TEM, which can provide direct visualization of the spatial distribution of the organoclay. Thin film samples of epoxy/organoclay nanocomposites with 5 wt% organoclay (about 100 nm thick) were cut from the specimens using a Reichert-Jung Ultracut E microtome, and the associated morphology was imaged using a JEOL 200CX transmission electron microscope at an accelerating voltage of 120 kV. Two different magnifications, 50k, and 200k, were taken for the observations, and the respective results are shown in Fig. 2(a) and (b). At low magnification, it was found that in some regions the clay is aggregated in the form of cluster structures. However, in other regions, no distinct clay platelets are observed. The micrographic observations indicate that the platelets are not dispersed and distributed homogeneously in the nanocomposites. According to the higher magnification micrographics, the interlayer spacing of the organoclay was estimated at 5 nm as indicated by the arrows in Fig. 2(b). Moreover, few exfoliated organoclay layers were found individually in the nanocomposites. Thus, based on the XRD measurements and TEM observations, it is suggested that the present samples could be regarded as intercalated nanocomposites.

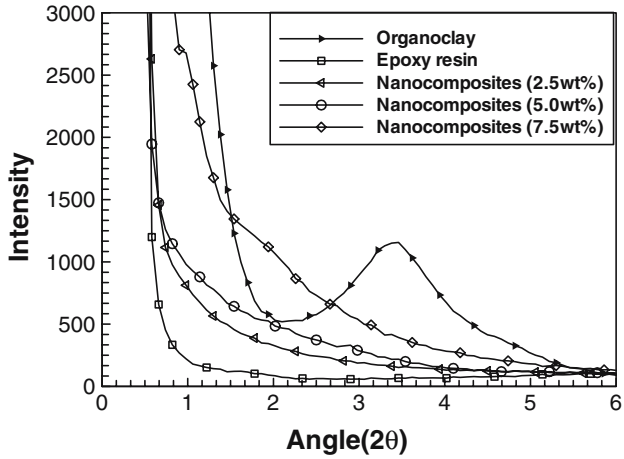

Fig. 1 X-ray diffractions of organoclay, neat epoxy and nanocomposites

Experiment

Tensile tests of epoxy/organoclay nanocomposites

To determine the organoclay effect on the mechanical properties of epoxy resin, nanocomposites containing three different loadings of organoclay, 2.5, 5 and 7.5%

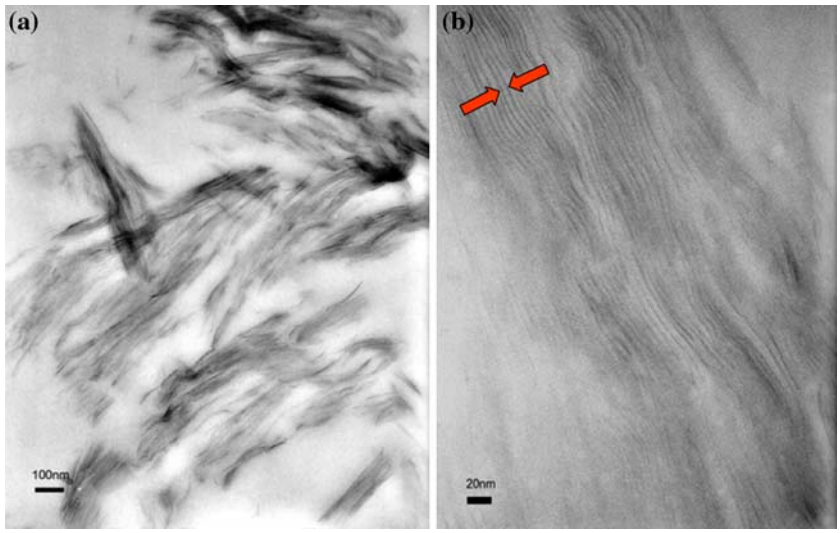

Fig. 2 TEM micrographics for the epoxy/organoclay nanocomposites with 5 wt% organoclay ((**a**) 50,000 magnification, (**b**) 200,000 magnification)

by weight, were tested in tension. Coupon specimens as shown in Fig. 3 were fabricated from the pre-designed mold with Teflon coating on the surface and then employed for tensile tests. The experiments were conducted on a hydraulic MTS machine with stroke control at a strain rate of 10^{-4}/s. Back-to-back strain gauges were mounted on the center of the specimens to eliminate the possible bending effect and to record the strain history during the tensile tests. The corresponding stress histories were obtained from the load cell embedded on the loading fixture. Figure 4 demonstrates the stress and strain curves for the pure epoxy and organoclay/epoxy material systems. The Young's moduli of the samples obtained from Fig. 1 are summarized in Table 1. It was revealed that stiffness increases along with the increase of the organoclay loadings. However, the corresponding failure strains decrease when the organoclay loadings increase. These phenomena imply that the inclusion of organoclay may enhance the stiffness of the epoxy resins but sacrifice their corresponding ductility.

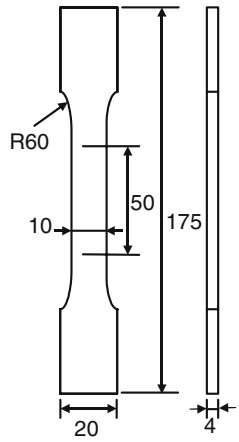

Fig. 3 Specimen configurations for tensile tests (unit: mm)

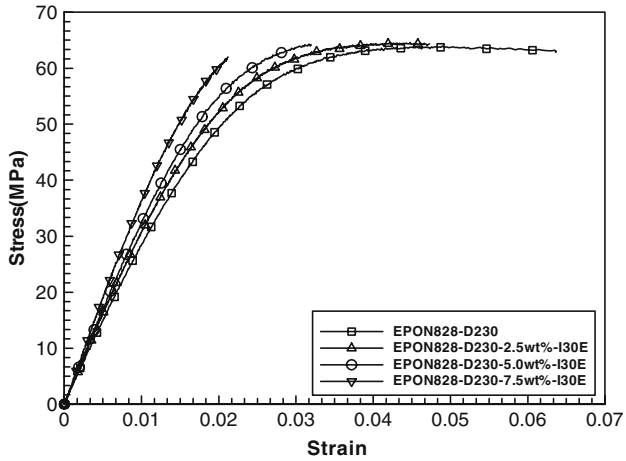

Fig. 4 Stress and strain curves for neat epoxy and nanocomposites with three different loadings of organoclay

Table 1 Young's modulus of epoxy nanocomposites with different organoclay loadings

Materials	Young's modulus (GPa)	Enhancement ratio (%)
Epoxy resin	3.0	
Nanocomposites (2.5 wt% organoclay)	3.3	11
Nanocomposites (5.0 wt% organoclay)	3.5	18
Nanocomposites (7.5 wt% organoclay)	3.9	29

Transverse compressive test of fiber nanocomposites

Block glass/epoxy nanocomposite specimens with dimension of $10 \times 6 \times 6$ mm were employed for compression tests. The block specimens were cut from 18-ply unidirectional glass/epoxy nanocomposites using a diamond wheel and then lapped on a lapping machine with 15 μm abrasive slurry to achieve smooth, flat loading surfaces. Compressive loading was applied on the specimens in the transverse direction (10 mm direction) by using a servo-hydraulic MTS machine. A self-adjusting device, as shown in Fig. 5, was used to eliminate potential bending and also to ensure the specimen be in full contact with the loading surfaces. The contact interface between the specimens and the loading fixture was lubricated to reduce friction. During the test, the applied load and displacement histories were recorded using a LabView with a personal computer. The associated peak values in the loading curves are considered to be the failure stress of the specimens.

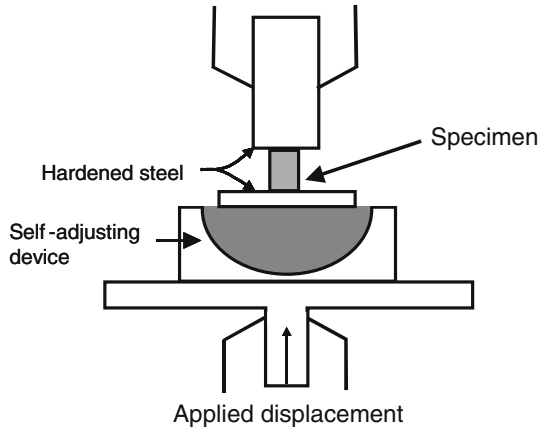

Fig. 5 Compression test for block glass/epoxy nanocomposite specimens

Results and discussion

The failure specimens for glass/epoxy composites and glass/epoxy nanocomposites with 5% concentration of organoclay are illustrated, respectively, in Fig. 6. In both material systems, the failure of the specimens is dominated by out-of-plane shear failure occurring on the plane orientated around 36° with respect to the loading direction. The transverse compressive strength of glass/epoxy nanocomposites was plotted versus the organoclay concentrations in Fig. 7. It is of note that for each organoclay concentration, four specimens were tested. The average values of the transverse compressive strengths obtained from different specimens associated with the same organoclay loading are listed in Table 2. It appears that for glass/epoxy nanocomposites, their failure stresses are relatively higher than those of conventional ones without any organoclay included. Moreover, transverse compressive strength increases with the increase of organoclay concentrations up to 5%; thereafter, it decreases. In order to further realize the increased behavior of transverse compressive strength, the failure surfaces of the specimens were examined closely using SEM. Figure 8 shows the SEM micrographic of glass/epoxy

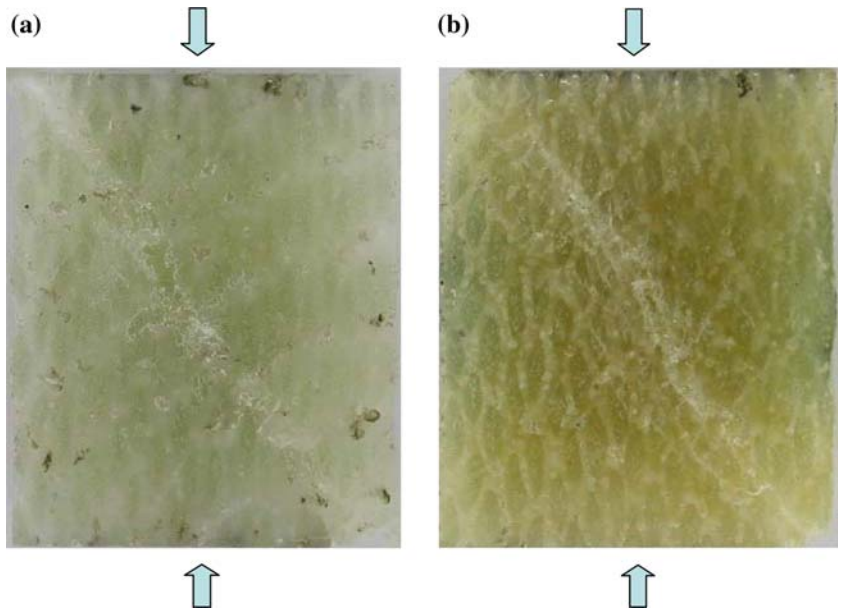

Fig. 6 Out-of-plane shear failure mechanisms ((**a**) glass/epoxy composites, (**b**) glass/epoxy nanocomposites with 5 wt% organoclay)

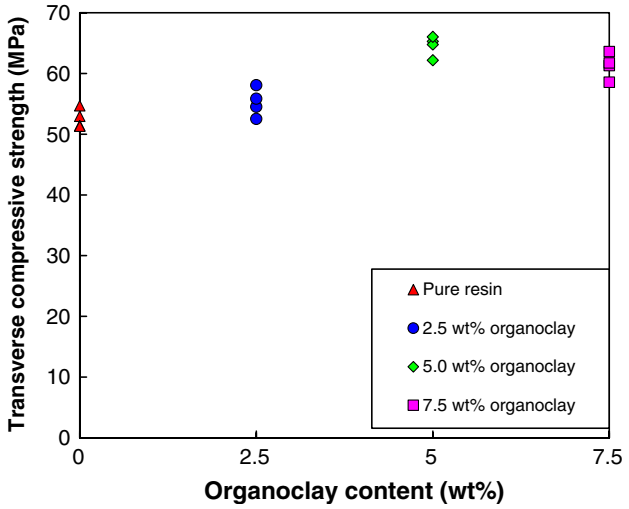

Fig. 7 Transverse compressive strength of glass/epoxy nanocomposites with different organoclay concentrations

Table 2 Transverse compressive strength of glass/epoxy nanocomposites with different organoclay loadings

Clay content (wt%)	Transverse compressive strength (MPa)	Improvement (%)
0	53	
2.5	55	4
5.0	66	24
7.5	61	15

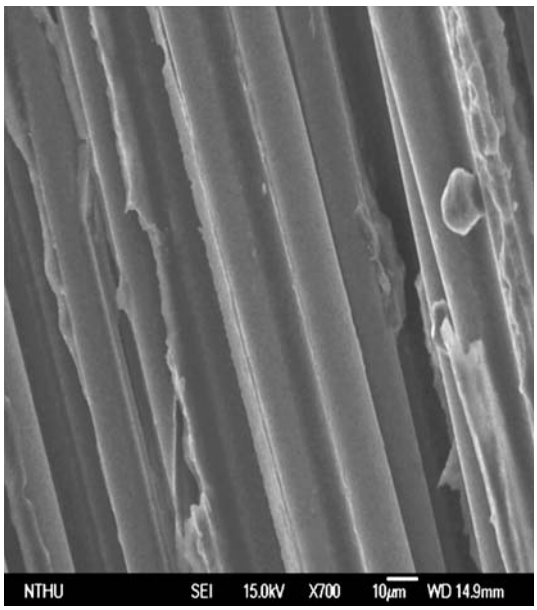

Fig. 8 SEM micrographics on the failure surfaces of the specimens glass/epoxy nanocomposites with 5 wt% organoclay loading

nanocomposites with 5 wt% organoclay. Results show that smooth fiber surfaces as well as matrix grooves are clearly found on the failure surfaces. In general, for fiber composites subjected to transverse compressive loading, failure could be dominated by matrix failure or fiber and matrix interfacial debonding depending on the relative strength of the matrix and the interfacial bonding. According to SEM observations, it seems that for the glass/epoxy nanocomposites, interfacial debonding between the glass fibers and the surrounding matrix is the main failure mechanism rather than the matrix failure. In addition, for conventional glass/epoxy composites, the similar characteristic of interfacial debonding was also observed on the failure surfaces. Therefore, the corresponding improvement of transverse compressive strength of the nanocomposites could be a result of enhanced interfacial bonding promoted by the organoclay. It is notable that when the organoclay was incorporated with the epoxy resin, due to the interaction of the organoclay and the polymer molecules, the morphology of the epoxy was changed. Moreover, the long alkyl chains attached on the surfaces of the organoclay may provide additional bonding to the fibers. In order to fully understand the organoclay effect on interfacial bonding, it is necessary to invoke molecular mechanics to study the interaction between epoxy resin and organoclay in conjunction with fibers.

However, for nanocomposites with 7.5% organoclay, failure stress is on the decline. In general, when the organoclay loading is increased, the viscosity of the compound becomes relatively higher. It is difficult to fully disperse the clay within the epoxy resin; thus, more defects could be generated during the fabrication process. Reduction behaviors in epoxy nanocomposites with higher organoclay loadings have also been observed in other polymer nanocomposites [14].

Conclusions

Epoxy/organoclay nanocomposites and unidirectional glass fiber/epoxy nanocomposites were fabricated through sonication with a vacuum hand lay-up process. Based on tensile tests on epoxy nanocomposites, results indicate that organoclay can increase the stiffness of epoxy resins without sacrificing their tensile strength. However, the corresponding failure strain decreases with the increase of organoclay concentrations. According to the transverse compressive failure test on unidirectional glass/epoxy nanocomposites, failure stress increases when the organoclay concentration increases up to 5%. Moreover, the main failure mode

for all tested specimens is fiber/matrix debonding. The corresponding increments in failure stresses could be due to the enhanced interfacial bonding between fiber and matrix promoted by the organoclay. Ultimately, it was concluded that the dispersion of organoclay in epoxy not only increases the stiffness of the epoxy resin but also enhances its interfacial adhesion to the fibers.

Acknowledgment This research was supported by the National Science Council, Taiwan under the Contract No. NSC 92-2212-E-009-029 to National Chiao Tung University.

References

1. Collings TA (1974) Composites 5(3):108
2. Bazhenov SL, Kozey VV (1991) J Mater Sci 26(10):2677
3. Lowe A (1996) J Mater Sci 31(4):1005
4. Thostenson ET, Li C, Chou TW (2005) Compos Sci Technol 65(3–4):491
5. Pinnavaia TJ, Beall GW (2000) In: Polymer-Clay Nanocomposites. John Wiley & Sons, New York
6. Usuki A, Kawasumi M, Kojima Y, Okada A, Kurauchi T, Kamigaito O (1993) J Mater Res 8(5):1174
7. Usuki A, Kojima Y, Kawasumi M, Okada A, Fukushima Y, Kurauchi T, Kamigaito O (1993) J Mater Res 8(5):1179
8. Cho JW, Paul DR (2001) Polymer 42(3):1083
9. Chin IJ, Thurn-Albrecht T, Kim HC, Russell TP, Wang J (2001) Polymer 42(13):5947
10. Ratna D, Manoj NR, Varley R, Singh Raman RK, Simon GP (2003) Polym Int 52(9):1403
11. Yano K, Usuki A, Okada A, Kurauchi T, Kamigaito O (1993) J Polym Sci A Polym Chem 31(10):2493
12. Dennis HR, Hunter DL, Chang D, Kim S, White JL, Cho JW, Paul DR (2001) Polymer 42(23):9513
13. Okada A, Usuki A (1995) Mater Sci Eng C 3(2):109
14. Haque A, Shamsuzzoha M, Huussain F, Dean D (2003) J Compos Mater 37(20):1821
15. Becker O, Varley RJ, Simon GP (2003) J Mater Sci Lett 22(20):1411
16. Technical data sheet, Nanocor Inc
17. Liu T, Tjiu WC, Tong Y, He C, Goh SS (2004) J Appl Sci 94(3):1236